

# Identifying Water Stress in Chickpea Plant by Analyzing Progressive Changes in Shoot Images using Deep Learning

Shiva Azimi, Rohan Wadhawan, *Student Member, IEEE*, and Tapan k. Gandhi, *Member, IEEE*,

**Abstract**—To meet the needs of a growing world population, we need to increase the global agricultural yields by employing modern, precision, and automated farming methods. In the recent decade, high-throughput plant phenotyping techniques, which combine non-invasive image analysis and machine learning, have been successfully applied to identify and quantify plant health and diseases. However, these image-based machine learning usually do not consider plant stress's progressive or temporal nature. This time-invariant approach also requires images showing severe signs of stress to ensure high confidence detections, thereby reducing this approach's feasibility for early detection and recovery of plants under stress. In order to overcome the problem mentioned above, we propose a temporal analysis of the visual changes induced in the plant due to stress and apply it for the specific case of water stress identification in Chickpea plant shoot images. For this, we have considered an image dataset of two chickpea varieties JG-62 and Pusa-372, under three water stress conditions; control, young seedling, and before flowering, captured over five months. We then develop an LSTM-CNN architecture to learn visual-temporal patterns from this dataset and predict the water stress category with high confidence. To establish a baseline context, we also conduct a comparative analysis of the CNN architecture used in the proposed model with the other CNN techniques used for the time-invariant classification of water stress. The results reveal that our proposed LSTM-CNN model has resulted in the ceiling level classification performance of 98.52% on JG-62 and 97.78% on Pusa-372 and the chickpea plant data. Lastly, we perform an ablation study to determine the LSTM-CNN model's performance on decreasing the amount of temporal session data used for training.

**Index Terms**—Computer vision, CNN, deep learning, plant phenotyping, water stress.

## I. INTRODUCTION

IT has been estimated that agricultural production should be doubled by 2050 in order to meet the demands of a growing world population. Achieving this goal poses a serious challenge to farming as the current agricultural production growth rate of 1.3% per annum is below the population growth rate [1]. To achieve the required agricultural growth rate, we require modern agricultural practices that focus more on precision and automated farming. In turn, this will employ a wide array of Internet of Things (IoT) sensors that measure soil conditions and imaging devices that keep track of specific traits such as color, size, and shape of the crops [2]. Furthermore,

we need to take a multidisciplinary approach that merges plant science, robotics, computer vision, and environmental sciences. Plant phenotyping is one such method that deals with the measurement of observable traits of a plant in reaction to genetic and environmental changes and has a large number of applications in plant science including plant breeding, quality assessments, and stress identification. Computer vision-based plant phenomics has a significant role in precision farming as it provides easy, fast, and highly automated methods for plant health and growth monitoring [3]. Additionally, it has been used for other tasks such as determining whether a plant is a crop or a weed and the soil's chemical content using near-infrared and hyperspectral imaging.

This paper focuses on abiotic stresses that result from the action of external environmental factors and often adversely affect agricultural productivity. Water and nitrogen stresses are the two most crucial abiotic stresses in plants that can change plants' physiological traits. The effect of water-induced stresses, which is a consequence of excessive or inadequate watering content in the soil, inhibits photosynthesis, and plants' growth. To better manage water stress and minimize crop loss resulting from it, we need to develop methods to quickly evaluate water stress without damaging the plants [4].

Most manual plant phenotyping approaches are costly, time-consuming, destructive, and cumbersome, thereby necessitating the development and use of high-throughput, non-invasive, and image-based plant phenotyping techniques to identify the stress levels in plants. These methods are fast, highly automated, and more accurate. Further, image-based plant phenotyping can be conducted inside a laboratory, inside a controlled chamber room, or on the field [5], [6]. These phenotyping techniques include two fundamental steps: the data acquisition step and the data analysis-inference step. With the recent developments in computer vision and object detection, capturing high-resolution images in both the visible and the hyperspectral has become straightforward and expedient [7], [8]. However, reliable and efficient data acquisition and processing methods often require expertise in biology, mathematics, and computer vision [9].

Moreover, phenotyping applications usually involve processing and analysis of a huge amount of data. Machine Learning (ML) methods have been proven to be quite efficient in the analysis of big data in research areas such as health and economics [10]. However, the traditional ML techniques suffer from the limitation imposed by hand-crafted features. These hand-crafted features often lack generality and are

Sh. Azimi, R. Wadhawan and T.K.Gandhi are with the Department of Electrical Engineering, Indian Institute of Technology-Delhi, New Delhi 110016, India. (\* Sh. Azimi and R. Wadhawan are co-first authors.) (e-mails: shiva.azimi@yahoo.com, rohanwadhawan7@gmail.com, and tgandhi@ee.iitd.ac.in).

unable to model complex features. This inherent limitation of the classical ML techniques has shifted the focus on Deep Learning (DL) based approaches to ML [11].

One such DL architecture commonly used in various computer vision tasks is the Convolutional Neural Network (CNN) [12]. CNNs possess convolutional layers for detecting visual features from images [13]. Further, it has been applied in several computer vision applications such as life sciences, medicine, and farming [14], [15]. It has also been widely employed for classifying plants and leaves in farming [16], [17]. DL techniques have also been used in related applications like counting the number of seeds per pod for soybeans [18], the number of wheat ears under field conditions [19], plant identification [20], identification of plant diseases [21], etc. Moreover, DL-based predictive methods have been applied in the farming domain, such as finding out future farming parameters - produce estimation [22], the soil moisture content in the field [23], and crop weather requirements [24].

Even though CNN has been proven very promising for image-based stress detection and classification in plants [25], it suffers from the following limitation. In this approach, plant images taken at different moments in time are considered to be equivalent. However, visual changes introduced due to stress does not become discernible immediately after stress; instead, this change is progressive. Due to CNN's time-invariant nature, it is unable to classify a stress condition with high confidence [25], [26]. This time-invariant approach also requires images showing severe signs of stress to ensure high confidence detections, thereby reducing this approach's feasibility for early detection and recovery of plants under stress. Therefore, there is a need for a technique that analyses this progressive visual change in stressed plants. This technique should classify stress with high confidence, even when available plant images do not show a sign of severe stress, as it can help us to identify stress in the plants at an early stage.

This paper aims to validate the need for temporal analysis and demonstrate its superiority over the time-invariant CNN technique for plant water stress (water deficiency) phenotyping. With this objective in mind, we make the following contributions in this paper:

- As there are no publicly available plant shoot image datasets of pulses that can be used to detect and classify moisture-related stress conditions, we have created a dataset of Chickpea plant shoot images for the experiments proposed in this article. The dataset comprises two varieties of chickpea plant species - JG-62 and Pusa-372. The shoot images under different water stress in India.
- We have proposed an LSTM-CNN architecture to learn visual-temporal patterns from the chickpea plant dataset. The proposed model has resulted in the ceiling level classification performance of **98.52%** on JG-62 and **97.78%** on Pusa-372 and the chickpea plant data.
- To establish a baseline context, we also conduct a comparative analysis of the CNN architecture used in the proposed model with the other CNN techniques used for time-invariant classification of water stress.
- We perform an ablation study to determine the LSTM-CNN model's performance on decreasing the amount of

temporal session data used for training.

The rest of this article is structured as follows. The dataset and DL techniques are presented in section 2. Section 3 provides the results. Finally, conclusions are provided in section 4.

## II. MATERIALS AND METHODS

In this section, we describe the dataset and methodology that we use for water stress identification in chickpea plants. First, we explain our dataset of chickpea plant shoot images and then we discuss the DL techniques used in this paper.

### A. Dataset

Most of the publicly available datasets for plant health analysis only contain images on plant leaves, which is significantly less informative than the entire plant shoot image. These datasets usually show plants under biotic stress, with very few covering plants under abiotic stress. Furthermore, to the best of our knowledge, there are no publicly available plant shoot image datasets of pulses, especially chickpea, to detect and classify moisture-related abiotic stress conditions. Therefore, it is necessary to create a database of plant shoot images of pulses with a sufficient number of images so that DL techniques can be applied. To this end, we created a new dataset of chickpea plant shoot images in the visible spectrum of light for this purpose.

Two varieties of chickpea strains (stress-tolerant Pusa-372 and stress-sensitive JG-62) were grown in individual plant pots in the control chamber room and observed over a period of five months for this experiment. The experiment was conducted in collaboration with plant scientists at the National Institute of Plant Genome Research (NIPGR). For both the varieties, plants were subjected to three different watering conditions, based on the water stress applied to them. The three watering conditions are Before Flowering (BF), in which a plant was not watered for 1 week after it was 2 weeks old; Young Seedling (YS), in which a plant was not watered for 1 week after it was 5 weeks old; Control (C), in which a plant was watered throughout. Water stress changes the physical structure of plants, such as shape and color. It also reduces plant height, plant biomass, and the number of branches, leaves, and fruits in chickpea plants. The plant shoot images were captured at a particular time once every three days. During each image capturing session, images were taken from eight different angles, at every 45°. Thus, in every session, we have captured 240 images across all the pots of both varieties. Overall, this dataset has a total of 7680 images. The black pot and the white background were seen in the image. However, DL techniques are able to avoid such invariant features existing in the context. Therefore, plant background segmentation is not compulsory for water stress identification. It would just decrease the number of features and, eventually, the computational cost.

### B. Deep Learning Approach

Over the years, DL techniques like CNNs have become state of the art for image classification. In our paper [27],

we employed a 23-layered custom CNN, and ResNet-18 [28] model for water stress classification from chickpea plant shoot images. The ResNet-18 classifier was able to achieve 84% and %86 accuracy on (*Pusa* – 372) and (*JG* – 62), respectively. However, this approach enforced a simplifying assumption on the dataset by treating all images belonging to one class equivalent even if they were taken at different times. Furthermore, water stress is introduced after 2 weeks, due to which the images up to that point across all the three conditions are similar to one another, thereby adding noise to the dataset. Despite this noise, the CNN classifier is robust enough to analyze water-stressed plants’ patterns with high accuracy. However, we believe that time-series analysis of the plant shoots’ visual features will remove this noise and produce better results.

Long Short Term Memory (LSTM) [29] networks have become a state-of-the-art technique for sequence learning problems like time series analysis. Moreover, LSTM and CNN combined have also been successfully used in tasks requiring sequence learning of visual features, like video classification and activity recognition in videos [30], [31]. Our task shares similarities with activity classification in videos that predicts which activity is being performed by analyzing visual changes over time. Similarly, we need to ascertain temporal patterns resulting from visual changes induced in the chickpea plant’s shoot due to water-stress. Thus, we propose an LSTM-CNN network to predict water stress in chickpea plants. In this architecture, CNN pre-trained on ImageNet data extracts visual features from the chickpea plant shoot images. Then, the LSTM analyses these features over time to predict the plant’s water stress condition. We also compare our previous time-invariant approach for water stress classification in chickpea plants [27] with our proposed LSTM-CNN time-series approach. To simulate time-invariant classification, we fine-tune the pre-trained CNN network, which is used for feature extraction in our proposed LSTM-CNN network, on our dataset. Then, we pass the image features extracted by the above-fine-tuned network through dense neural network layers for water stress classification in chickpea plants. We describe the architectures, input processing, and neural network training in the subsequent sections.

1) *CNN*: Several CNN architectures have been developed over time. In this paper, we have used VGG16 [32] and Inception-V3 [33] architectures for the following two purposes. Firstly, we fine-tune models of these architectures pre-trained on the ImageNet dataset [34] and use them for time-invariant classification of chickpea plants under water stress conditions. Secondly, we use these models as feature extractors in our proposed LSTM-CNN architecture.

**VGG16**: VGG16 architecture has achieved state-of-art accuracy for image classification on the ImageNet dataset in the past. This architecture introduces the concept of stacking smaller convolutional kernels to produce an effective receptive field. This technique also decreased the total number of parameters to achieve the same receptive field and increased non-linearity due to activation across multiple stacked layers. This model was deeper and less wide than GoogLeNet (Inception-V1) [35] proposed around the same time. Although VGG16

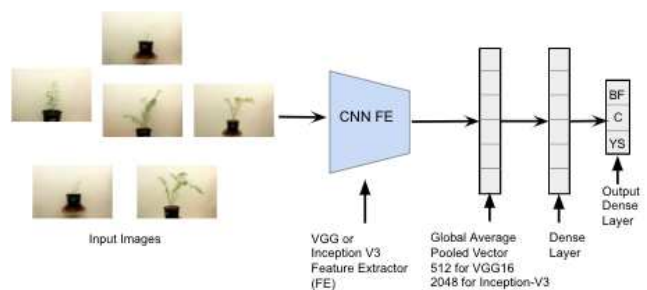


Fig. 1. Time-Invariant CNN architecture used for water stress classification (BF, YS, C) in chickpea plants shoot images. In this diagram, we have used images of JG-62 chickpea species.

performs better than GoogLeNet on the ImageNet dataset, it is more computationally complex and has a larger requirement of compute, memory, and storage resources.

**Inception-V3**: Inception-V3 architecture proposed as an improvement over its predecessors (Inception-V1 and Inception-V2) has achieved state-of-the-art accuracy for image classification on ImageNet dataset in the past. Some of the essential features of this model are: it is deeper, avoids representational bottlenecks, especially early in the network, maintains higher dimensional representation, spatial aggregation on the lower dimension, balance width, and depth of the network. It further reduces the computational complexity, both in terms of the number of parameters and cost of resources (memory and storage) compared to Inception-V1 and Inception-V2 architectures, and increases classification accuracy. Inception-V3 performs better than VGG16 on the ImageNet dataset.

2) *Time-Invariant CNN Architecture*: This network is used to perform a time-invariant classification analysis for identifying water stress in chickpea plant shoot images. For this purpose, we use the convolutional base of the VGG16 and Inception-V3 network and remove the corresponding dense layers. Then, we perform Global Average Pooling [36] after the last Max Pooling layer. Global Average Pooling is preferred over fully connected layers for flattening the feature maps to a linear vector because it is more native to the convolution structure and enforces correspondences between feature maps and categories. Further, this layer has no parameters to optimize, which reduces the chances of over-fitting and is also more robust to the input’s spatial translation. Finally, we add two dense layers after global average pooling, the first one has 512 dimensions, and the following is the output layer with three dimensions, equal to the number of classes, as shown in Fig. 1. We initialize each dense layer using the Glorot uniform initializer [37] and use Softmax activation in the final output Dense layer (Equation ??).

3) *LSTM*: LSTM is an improvement over the artificial recurrent neural network (RNN) architecture [29]. Unlike RNN, LSTM can learn long-term dependencies and preserve the useful temporal information for an extended period. A standard

LSTM unit comprises a cell, an input gate, an output gate, and a forget gate. The cell remembers values over arbitrary time intervals, and the three gates regulate the flow of information into and out of the cell. The equations for an LSTM are defined as:

$$f_t = \sigma_g(W_f x_t + U_f h_{t-1} + b_f) \quad (1)$$

$$i_t = \sigma_g(W_i x_t + U_i h_{t-1} + b_i) \quad (2)$$

$$o_t = \sigma_g(W_o x_t + U_o h_{t-1} + b_o) \quad (3)$$

$$\tilde{c}_t = \sigma_c(W_c x_t + U_c h_{t-1} + b_c) \quad (4)$$

$$c_t = f_t \odot c_{t-1} + i_t \odot \tilde{c}_t \quad (5)$$

$$h_t = o_t \odot \sigma_h(c_t) \quad (6)$$

Where,  $x_t$ ,  $f_t$ ,  $i_t$ ,  $o_t$ ,  $\tilde{c}_t$ ,  $c_t$  and  $h_t$  define as input, forget gate, input gate, output gate, cell input, cell state and hidden state vector respectively. The bias, weight matrices and recurrent connections are represented as  $b$ ,  $W$  and  $U$ , respectively. In addition,  $\odot$  denotes an element-wise multiplication.

4) *Proposed LSTM-CNN Architecture:* Our LSTM-CNN architecture consists of two main parts: CNN image feature extractor and LSTM to predict water stress category from the extracted features. The architecture is shown in Fig. 2.

**CNN feature extractor:** We use VGG16 and Inception-V3 models pre-trained on ImageNet dataset to extract visual features from chickpea plant images. We employ two different feature pre-trained extractors to determine if our approach is CNN architecture-dependent. In both the models, we remove the dense layers and apply Global Average Pooling after the final Max-Pooling layer to obtain 1D vectors of size 512 and 2048 for VGG16 and Inception-V3, respectively. These vectors are used as input for the LSTM cells, as shown in Fig. 2.

**LSTM predictor:** In our LSTM network, the number of sequentially connected cells is equal to the number of session data used for prediction, as shown in Fig. 2. This dynamic length of the LSTM network helps us analyze the effect of the number of data sessions on the prediction performance metrics - Accuracy, Macro Sensitivity, Macro Specificity, and Macro Precision. An ablation study on the same is reported in section III-C. The LSTM network output is fed into a Dense Layer of size 512 dimension, which is connected to the Dense output layer of size 3, that is, equal to the number of water stress categories. We initialize each dense layer using the Glorot uniform initializer and use Softmax activation in the final output Dense layer.

5) *Input Processing: LSTM-CNN Network:* This section describes input dataset preparation for our proposed LSTM-CNN network. Our dataset consists of two chickpea species: *JG* – 62 and *Pusa* – 372. We have 15 pots per species and 5 per water stress category - young seedling, control, and before flowering. For each pot, we have 32 sessions of data. Lastly, in each session, we take eight photographs of the plant, one at every 45o. If we consider plant images at one of the above angles, we obtain 15 data samples, one for each pot. Each sample consists of 32 images, one from every photo session. To ensure the robustness of classification, we consider photographs at all angles, such that all images of one data sample have been taken from the same angle. Thus, for both JG-62 and Pusa-372, we have 120 data samples each, in which there are 40 samples for each water stress category. We use RGB input images of size (224,224,3) and perform CNN network-specific image preprocessing on them before feeding them to our LSTM-CNN network.

**Time-Invariant CNN Network:** This section describes input data preparation for fine-tuning pre-trained VGG16 and Inception-V3 CNN networks for time-invariant comparison with our previous method [27]. In this case, we equivalently treat all images of a given plant taken at different points in time. Thus, we have 1280 images per category and 3840 in total for each species. We use RGB input images of size (224,224,3) and perform network-specific image preprocessing before feeding them to the corresponding CNN network for fine-tuning.

6) *Training:* In this paper, we use 5-fold stratified cross-validation to train and evaluate our networks. In other words, we divide the entire dataset into 5 equivalent subsets and train a model on 4 out of 5 of them. Then, we test on the remaining subset such that each subset acts as a test set once. In other words, we train 5 models on the entire dataset. Finally, we report the average scores across all 5 models for each performance metric - Accuracy, Macro-Sensitivity, Macro-Specificity, and Macro-Precision. We also repeat the cross-validation process 10 times to ensure robustness of the reported scores.

In our LSTM-CNN network, we only train the LSTM and the dense layer. We do not train the CNN network because of the limited availability of data. The LSTM network trained on 32 sessions data has about **2.4M** and **35M** trainable parameters with VGG16 and Inception-V3 feature extractors, respectively. However, if we make all the CNN networks trainable in the 32 cell LSTM, the CNN networks alone will contribute to **471M** or **696M** parameters (VGG16 or Inception-V3). Now, comparing the number of parameters to the **578M** pixels in 3840, 224x224x3 images of each plant species, we observe that the numerical parameters are almost the same or more than the number of pixels. Due to this, the network will be inclined to learn the input data rather than the visual pattern from it, thereby over-fitting the dataset. Thus, we only train the LSTM network. On the other hand, to simulate time-invariant classification, we fine-tune the pre-trained VGG16 and Inception-V3 networks on our dataset.

We train and fine-tune the neural networks using the back-propagation technique [38] and formulate a categorical cross-

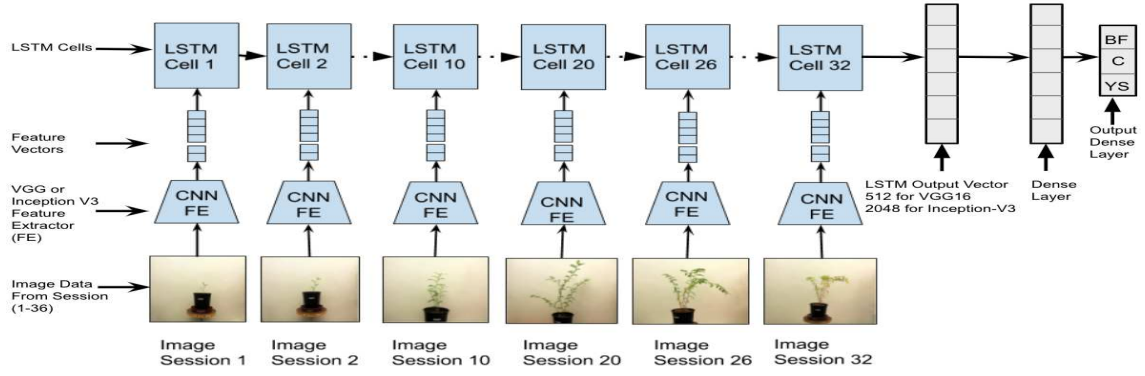


Fig. 2. LSTM-CNN architecture used for predicting water stress classification (BF,YS,C) in chickpea plant. Number of LSTM cells equals the number of session data used. In this diagram, the images of a JG plant samples over 32 session are used.

entropy loss for water stress condition classification. The training is performed using a mini-batch size of 32 images and neural network weights are optimized using Adam optimizer [39] with learning rate  $\alpha = 0.0001$  and the other optimizer parameters being  $\{\beta_1 = 0.9, \beta_2 = 0.999, \epsilon = 10^{-7}\}$ .

$$\text{Categorical Cross Entropy} = -\log \left( \frac{\exp^{s_p}}{\sum_j^C \exp^{s_j}} \right) \quad (7)$$

Where  $s_p$  is the score of the positive class,  $s_j$  is the score of the class  $j$ ,  $C$  is the number of classes,  $Classes = \{Before Flowering, Control, Young Seedling\}$ ,

**Training Environment** We use Tensorflow and Keras DL framework to train our models and train them on a single Nvidia Tesla K80 GPU.

### C. Performance Evaluation Metrics

We report the confusion matrices for each LSTM-CNN model. Mathematically they are defined as;

$$\text{Average Accuracy} = \frac{\sum_i^C \frac{Tp_i + Tn_i}{Tp_i + Tn_i + Fp_i + Fn_i}}{\sum_j^C 1} \quad (8)$$

$$\text{Macro - Sensitivity} = \frac{\sum_i^C \frac{Tp_i}{Tp_i + Fn_i}}{\sum_j^C 1} \quad (9)$$

$$\text{Macro - Specificity} = \frac{\sum_i^C \frac{Tn_i}{Tn_i + Fp_i}}{\sum_j^C 1} \quad (10)$$

$$\text{Macro - Precision} = \frac{\sum_i^C \frac{Tp_i}{Tp_i + Fp_i}}{\sum_j^C 1} \quad (11)$$

Here,  $Tp_i$  represents the true positives;  $Tn_i$  represents the true negatives;  $Fp_i$  represents the false positives;  $Fn_i$  represents the false negatives with respect to the actual and predicted water stress class; such that  $i, j \in Classes$  and  $Classes = \{Before Flowering, Control, Young Seedling\}$ , and  $C$  is the number of classes.

TABLE I  
PERFORMANCE METRICS FOR WATER STRESS CLASSIFICATION USING TIME-INVARIANT TRAINING OF CNN MODELS ON JG-62 AND PUSA-372 VARIETIES OF CHICKPEA PLANTS (ACC: ACCURACY (IN %), SE: SENSITIVITY, SP: SPECIFICITY, PRE: PRECISION).

Chickpea Species	CNN Model	Acc	Se	Sp	Pre
<b>JG - 62</b>	VGG16	70.96	70.96	87.37	70.59
	Inception-V3	80.99	80.99	91.35	81.11
	CNN [27]	78.00	78.00	89.00	77.00
	ResNet-18 [27]	86.00	86.00	93.00	86.00
<b>Pusa - 372</b>	VGG16	72.14	72.14	87.34	76.90
	Inception-V3	72.14	72.14	87.34	76.90
	CNN [27]	76.00	76.00	88.00	75.00
	ResNet-18 [27]	84.00	84.00	92.00	84.00

## III. EXPERIMENTAL RESULTS

In this section, we describe the three experiments performed on the dataset. The first experiment examines VGG16 and Inception-V3 for water stress classification from chickpea plant shoot images by performing time-invariant training, similar to our previously used technique [27]. This experiment's objective is to demonstrate that changing the CNN network does not improve performance metric values due to the problem induced from equally treating all images belonging to a class, taken at different times. Then, in our second experiment, we train and evaluate LSTM-CNN models to investigate the effectiveness of temporal analysis of the visual features extracted from plant shoot images in terms of the four performance metrics employed in this paper. Lastly, we perform an ablation study to determine how the LSTM-CNN model's effectiveness changes on uniformly decreasing the amount of session data used for training the models.

### A. Time-Invariant Analysis

In this experiment, we conduct 5-fold stratified cross-validation training of VGG16 and Inception-V3 CNN models on the 3840 samples of each chickpea variety in our dataset. Before training, the images go through network-specific input processing. Each model represents one of the plant-variety and feature extractor pair, that is, JG-62 with VGG16 and Inception-V3 network and similarly for Pusa-372. We train the

TABLE II  
PERFORMANCE METRICS FOR LSTM-CNN MODELS ON JG-62 AND PUSA-372 VARIETIES OF CHICKPEA PLANTS USING VGG16 AND INCEPTION-V3, CNN FEATURE EXTRACTOR (ACC: ACCURACY (IN %), SE: SENSITIVITY, SP: SPECIFICITY, PRE: PRECISION).

Chickpea Species	CNN Model	Acc	Se	Sp	Pre
JG - 62	VGG16	98.32	0.9833	0.9916	0.9852
	Inception-V3	98.32	0.9833	0.9916	0.9852
Pusa - 372	VGG16	97.50	0.9749	0.9874	0.9778
	Inception-V3	97.50	0.9749	0.9874	0.9778

dense layers and fine-tune the convolution base of each model for 200 epochs. Then, we evaluate the performance metrics on the final models. The results are shown in Table I. We draw the following inferences from the result.

Firstly, we observe that VGG16 and Inception-V3 models' performance is similar to the performance of our previous techniques, that is, a custom-CNN architecture and ResNet-18 architecture, and the best results are achieved by the ResNet-18 model. Apart from the architectures, the other difference between the approaches mentioned above is the training parameters like the number of epochs and batch size. Secondly, we infer that VGG16 and Inception-V3 models' performance on JG images is better than Pusa images, which is consistent with our previous results [27], as shown in Table I. This can be attributed to the water-resistant nature of Pusa species and the water-sensitive nature of JG species. In other words, the visual changes introduced due to water stress are more prominent in the case of JG than Pusa, thus making it easier to classify JG images into the three water stress categories. Lastly, we observe that Inception-V3 models produced better results than VGG16 models across both chickpea species. This can be explained by relating these results with both these architectures' classification results on the ImageNet dataset. Inception-V3 outperforms VGG16 in both the top 1 and top 5 error rates (%) because it can extract better visual features [32], [33]. This suggests that image-based classification by transfer learning from Inception-V3 should be better than VGG16, consistent with the results shown in Table I. Therefore, time-invariant water-stress classification is network dependent.

### B. Temporal Analysis

In this experiment, we perform 5-fold stratified cross-validation training of four LSTM-CNN models on the 120 samples, each with 32 session images, from our dataset after performing the required input processing. Each model represents one of the plant-variety and feature extractor pair, that is, JG-62 with VGG16 and Inception-V3 network and similarly for Pusa-372. We train each model for 200 epochs and evaluate the performance metrics on the final models. The results are shown in Table II.

The results demonstrate that temporal analysis of visual changes in the chickpea plants, induced due to water stress, leads to better classification compared to time-invariant analysis shown in Table I. Additionally, each of the varieties' results is consistent for both feature extractors, showing that the proposed LSTM-CNN architecture is independent of the feature

		Predicted					Predicted		
		BF	C	YS			BF	C	YS
Actual	BF	1.0	0.0	0.0	Actual	BF	0.95	0.0	0.05
	C	0.0	1.0	0.0		C	0.0	1.0	0.0
	YS	0.05	0.0	0.95		YS	0.0	0.0	1.0

(a) JG - VGG16

		Predicted					Predicted		
		BF	C	YS			BF	C	YS
Actual	BF	1.0	0.0	0.0	Actual	BF	0.925	0.075	0.0
	C	0.0	1.0	0.0		C	0.0	1.0	0.0
	YS	0.0	0.075	0.925		YS	0.0	0.0	1.0

(c) Pusa - VGG16

		Predicted					Predicted		
		BF	C	YS			BF	C	YS
Actual	BF	1.0	0.0	0.0	Actual	BF	0.925	0.075	0.0
	C	0.0	1.0	0.0		C	0.0	1.0	0.0
	YS	0.0	0.075	0.925		YS	0.0	0.0	1.0

(d) Pusa - Inception-V3

Fig. 3. Confusion matrix depicting the results for LSTM-CNN model with VGG16 and Inception-V3 as the CNN feature extractor trained on 32 sessions of JG-62 and Pusa-372 species. Here, (a), (b), (c), and (d) represent the confusion matrices of the different possible species - feature extractor models.

extractor network. We observe that the LSTM-CNN performs better on JG-62 than Pusa-372. This observation corresponds to the inherent water stress sensitivity characteristics of these two chickpea varieties. JG is water stress-sensitive, thus producing more noticeable visual changes over time than Pusa, which is water stress-tolerant. This can also be seen from the time-invariant analysis results performed in our prior work and the baseline analysis reported in this paper, as shown in Table I. The confusion matrices for each model are shown in Fig. 3, where each cell's value represents the average probability across all the folds.

### C. Ablation Study

We perform an ablation study to determine the LSTM-CNN model's performance on decreasing the amount of session data used for training. In this study, we evaluate LSTM-CNN models corresponding to each chickpea plant species *JG - 62*, *Pusa - 372*, and CNN feature extractor *VGG16*, *Inception - V3* pair. We train 8 models for each pair, such that each model differs in the number of session data used. Starting from the 32nd session down to the 4th session, we reduce the number of sessions data by 4. A gap of 4 sessions was chosen as it provided the best solution for the tradeoff between the available computational resources and time for training models vs. the change in the performance metrics' value between two consecutive models. Moreover, Each model, out of a total of 32 models across the 4 possible LSTM-CNN model types, undergoes 5-fold stratified cross-validation training for 200 epochs. We report the results obtained in Table III and visualize the value of each performance metric vs. the number of session data in the graphs shown in Fig. 4.

We draw the following inferences from the result. Firstly, the graphs in Fig. 4 and Table III demonstrate that by decreasing the number of session data for training the model, we decrease its ability to discern water stress condition. Secondly,

TABLE III

ABLATION STUDY: PERFORMANCE METRICS FOR LSTM-CNN MODEL ON JG-62 AND PUSA-372 VARIETIES USING VGG16 AND INCEPTION-V3 IMAGE FEATURE EXTRACTOR (ACC: ACCURACY (IN %), SE: MACRO-SENSITIVITY, SP: MACRO-SPECIFICITY, PRE: MACRO-PRECISION) ON  $S_n$  SESSION DATA WHERE N REPRESENT IMAGES OF DATASET UP TO THE NTH SESSION. THE VALUE OF THE PERFORMANCE METRIC REPORTED IS THE AVERAGE VALUE AFTER 5-FOLD CROSS-VALIDATION.

Chickpea Species	Feature Extractor	Metric	S4	S8	S12	S16	S20	S24	S28	S32
JG - 62	VGG16	Acc	87.5	91.67	93.33	93.33	95.83	97.5	97.5	98.32
		Se	0.875	0.9167	0.9333	0.9333	0.9583	0.9749	0.9749	0.9833
		Sp	0.9375	0.9583	0.9662	0.9662	0.9791	0.9874	0.9874	0.9916
		Pre	0.8857	0.9267	0.9412	0.9557	0.963	0.9704	0.9778	0.9852
	Inception-V3	Acc	87.5	91.67	93.33	93.33	95.83	97.5	97.5	98.32
		Se	0.875	0.9167	0.9333	0.9333	0.9583	0.9749	0.9749	0.9833
		Sp	0.9375	0.9583	0.9662	0.9662	0.9791	0.9874	0.9874	0.9916
		Pre	0.8857	0.9267	0.9412	0.9557	0.963	0.9704	0.9778	0.9852
Pusa - 372	VGG16	Acc	83.33	87.5	91.67	93.33	95.83	96.66	96.66	97.5
		Se	0.8333	0.875	0.9167	0.9333	0.9583	0.9666	0.9666	0.9749
		Se	0.9167	0.9583	0.9583	0.9666	0.9791	0.9833	0.9833	0.9874
		Pre	0.8426	0.933	0.933	0.945	0.963	0.9704	0.9704	0.9778
	Inception-V3	Acc	87.5	93.33	94.99	95.83	96.66	96.66	97.5	97.5
		Se	0.8751	0.9083	0.9249	0.9583	0.9666	0.9666	0.9749	0.9749
		Sp	0.9375	0.9666	0.9707	0.9791	0.9833	0.9833	0.9874	0.9874
		Pre	0.8857	0.945	0.951	0.963	0.9704	0.9704	0.9778	0.9778

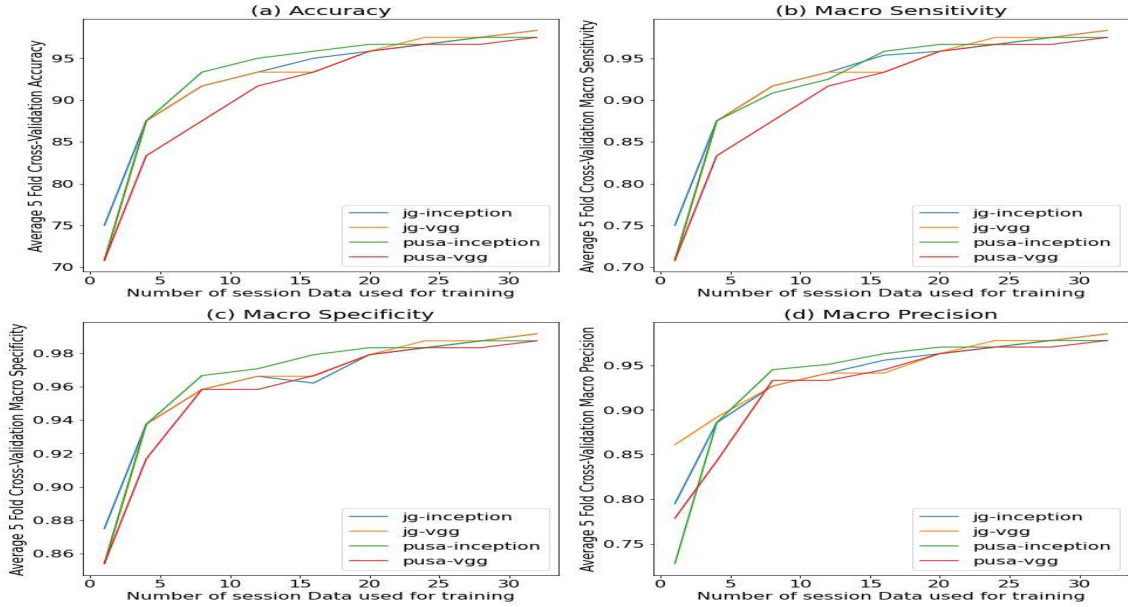


Fig. 4. Visualizing the accuracy, macro-sensitivity, macro-specificity, and macro-precision of models trained on different chickpea plant species - feature vector combination over the number of sessions data for training. Here accuracy, macro-sensitivity, macro-specificity, and macro-precision macro-precision is the average value of the 5 cross-validation fold represented in (a), (b), (c), and (d) respectively.

the performance metric curves (as shown in Fig 4) for a given plant species are similar for both the feature extractors. This shows that temporal analysis using LSTM-CNN models has negligible dependence on the CNN feature extractor used. On the contrary, the time-invariant classification of water stress depends on the CNN architectures employed, as shown in Table I. This observation further reinforces the merit of temporal analysis. Lastly, we also observe that these curves and final scores are consistent across both species, thereby demonstrating that temporal analysis performs well across

different chickpea plant species.

#### D. Computational Complexity

In this section, we report the time and space complexity of inference. To report the worst-case complexities, we utilize the models trained on 32 sessions of data, as these models have the maximum number of parameters. The inference time does not include time taken to load the 32 session images, pre-process the image, and load the model. In other words, we measure the time taken for feedforward propagation of the model. We

calculate the inference time on the Nvidia Tesla K80 GPU and Intel(R) Xeon(R) CPU for all three networks. A model with the VGG16 feature extractor takes **29ms** and **70ms** to predict the plant's water stress condition from its session data on the GPU and CPU, respectively. Similarly, A model with the Inception-V3 feature extractor takes **59ms** and **98ms** to predict the plant's water stress condition from its session data on the GPU and CPU, respectively. We find that model inference time for a model with the Inception-V3 feature extractor is higher than a one with the VGG16 feature extractor because the former has more number model parameters than the latter, as mentioned in section II-B6. Consequently, a model with the VGG16 feature extractor occupies approximately **28 MB** of space, which is less than the **397 MB** of space occupied by a model with the Inception-V3 feature extractor occupies approximately.

#### IV. CONCLUSION

In this study, we have focused on the temporal analysis of the visual changes induced in plants due to water stress. As there are no publicly available datasets of pulses plant shoot images, we first consolidated a new dataset of two varieties of chickpea shoot images dataset under different water stress conditions. We then proposed a novel DL model combining the CNN and an LSTM model to learn visual-temporal patterns for identifying moisture deficiency in plants with high confidence. The results of the time-invariant classification of water-stress in Chickpea plants revealed that this approach does not classify with high confidence, and its performance is convolutional neural network dependent. On the other hand, we observed the proposed LSTM-CNN model outperforms other time-invariant approaches for water stress classification in chickpea plant shoot images. The temporal analysis results also showed a negligible dependence on CNN feature extractor, which opens new avenues of research involving lightweight feature extractors. The classification performance also improved over the time-invariant approach by nearly 14% for both chickpea varieties. Additionally, the ablation study demonstrates that by decreasing the number of session data for training the model, we decrease its ability to discern water stress conditions, which is consistent with the progressive degrading changes induced in plants due to moisture deficiency over time. It demonstrates that temporal analysis using the LSTM-CNN model performs well across the different chickpea plant species and reinforces that it has negligible dependence on CNN feature extractors. Therefore, the proposed LSTM-CNN model can be used to develop in real-time monitoring of plant disease in IoT based applications to improve the agriculture yield. Future works will also be focused on proposing a better lightweight model that can be easily implemented on a simple computing platform. Besides, we intend to explore the use of deep learning for crop prediction for real-time applications in precision farming.

#### REFERENCES

[1] A. J. Challinor, J. Watson, D. B. Lobell, S. Howden, D. Smith, and N. Chhetri, "A meta-analysis of crop yield under climate change and adaptation," *Nature Climate Change*, vol. 4, no. 4, p. 287, 2014.

[2] D. Reynolds, J. Ball, A. Bauer, R. Davey, S. Griffiths, and J. Zhou, "Cropsight: a scalable and open-source information management system for distributed plant phenotyping and iot-based crop management," *Gigascience*, vol. 8, no. 3, p. giz009, 2019.

[3] D. I. Patrício and R. Rieder, "Computer vision and artificial intelligence in precision agriculture for grain crops: A systematic review," *Computers and electronics in agriculture*, vol. 153, pp. 69–81, 2018.

[4] V. Pandey and A. Shukla, "Acclimation and tolerance strategies of rice under drought stress," *Rice Science*, vol. 22, no. 4, pp. 147–161, 2015.

[5] G. Bai, Y. Ge, W. Hussain, P. S. Baenziger, and G. Graef, "A multi-sensor system for high throughput field phenotyping in soybean and wheat breeding," *Computers and Electronics in Agriculture*, vol. 128, pp. 181–192, 2016.

[6] R. Panwar, K. Goyal, N. Pandey, and N. Khanna, "Imaging system for classification of local flora of uttarakhand region," in *2014 International Conference on Power, Control and Embedded Systems (ICPCES)*. IEEE, 2014, pp. 1–6.

[7] K. Neumann, C. Klukas, S. Friedel, P. Rischbeck, D. Chen, A. Entzian, N. Stein, A. Graner, and B. Kilian, "Dissecting spatiotemporal biomass accumulation in barley under different water regimes using high-throughput image analysis," *Plant, cell & environment*, vol. 38, no. 10, pp. 1980–1996, 2015.

[8] M. S. M. Asaari, P. Mishra, S. Mertens, S. Dhondt, D. Inzé, N. Wuyts, and P. Scheunders, "Close-range hyperspectral image analysis for the early detection of stress responses in individual plants in a high-throughput phenotyping platform," *ISPRS journal of photogrammetry and remote sensing*, vol. 138, pp. 121–138, 2018.

[9] J. F. Humplík, D. Lazár, A. Husičková, and L. Spíchal, "Automated phenotyping of plant shoots using imaging methods for analysis of plant stress responses—a review," *Plant methods*, vol. 11, no. 1, p. 29, 2015.

[10] A. Singh, B. Ganapathysubramanian, A. K. Singh, and S. Sarkar, "Machine learning for high-throughput stress phenotyping in plants," *Trends in plant science*, vol. 21, no. 2, pp. 110–124, 2016.

[11] Y. LeCun, Y. Bengio, and G. Hinton, "Deep learning," *nature*, vol. 521, no. 7553, p. 436, 2015.

[12] Y. LeCun, B. E. Boser, J. S. Denker, D. Henderson, R. E. Howard, W. E. Hubbard, and L. D. Jackel, "Handwritten digit recognition with a back-propagation network," in *Advances in neural information processing systems*, 1990, pp. 396–404.

[13] Y. LeCun, L. Bottou, Y. Bengio, P. Haffner *et al.*, "Gradient-based learning applied to document recognition," *Proceedings of the IEEE*, vol. 86, no. 11, pp. 2278–2324, 1998.

[14] G. Litjens, T. Kooi, B. E. Bejnordi, A. A. A. Setio, F. Ciompi, M. Ghafoorian, J. A. Van Der Laak, B. Van Ginneken, and C. I. Sánchez, "A survey on deep learning in medical image analysis," *Medical image analysis*, vol. 42, pp. 60–88, 2017.

[15] A. Kamilaris and F. X. Prenafeta-Boldú, "Deep learning in agriculture: A survey," *Computers and electronics in agriculture*, vol. 147, pp. 70–90, 2018.

[16] S. H. Lee, C. S. Chan, S. J. Mayo, and P. Remagnino, "How deep learning extracts and learns leaf features for plant classification," *Pattern Recognition*, vol. 71, pp. 1–13, 2017.

[17] S. H. Lee, C. S. Chan, and P. Remagnino, "Multi-organ plant classification based on convolutional and recurrent neural networks," *IEEE Transactions on Image Processing*, vol. 27, no. 9, pp. 4287–4301, 2018.

[18] L. C. Uzal, G. L. Grinblat, R. Namías, M. G. Larese, J. Bianchi, E. Morandi, and P. M. Granitto, "Seed-per-pod estimation for plant breeding using deep learning," *Computers and electronics in agriculture*, vol. 150, pp. 196–204, 2018.

[19] S. Madec, X. Jin, H. Lu, B. De Solan, S. Liu, F. Duyme, E. Heritier, and F. Baret, "Ear density estimation from high resolution rgb imagery using deep learning technique," *Agricultural and Forest Meteorology*, vol. 264, pp. 225–234, 2019.

[20] Y. Sun, Y. Liu, G. Wang, and H. Zhang, "Deep learning for plant identification in natural environment," *Computational intelligence and neuroscience*, vol. 2017, 2017.

[21] J. G. A. Barbedo, "Plant disease identification from individual lesions and spots using deep learning," *Biosystems Engineering*, vol. 180, pp. 96–107, 2019.

[22] K. Kuwata and R. Shibasaki, "Estimating crop yields with deep learning and remotely sensed data," in *2015 IEEE International Geoscience and Remote Sensing Symposium (IGARSS)*. IEEE, 2015, pp. 858–861.

[23] L. Song, S. Prince, B. Valliyodan, T. Joshi, J. V. M. dos Santos, J. Wang, L. Lin, J. Wan, Y. Wang, D. Xu *et al.*, "Genome-wide transcriptome analysis of soybean primary root under varying water-deficit conditions," *BMC genomics*, vol. 17, no. 1, p. 57, 2016.



- [24] G. Sehgal, B. Gupta, K. Paneri, K. Singh, G. Sharma, and G. Shroff, "Crop planning using stochastic visual optimization," pp. 47–51, 2017.
- [25] S. Azimi, T. Kaur, and T. K. Gandhi, "A deep learning approach to measure stress level in plants due to nitrogen deficiency," *Measurement*, p. 108650, 2020.
- [26] Z. Gao, Z. Luo, W. Zhang, Z. Lv, and Y. Xu, "Deep learning application in plant stress imaging: a review," *AgriEngineering*, vol. 2, no. 3, pp. 430–446, 2020.
- [27] S. Azimi, T. Kaur, and T. K. Gandhi, "Water stress identification in chickpea plant shoot images using deep learning," p. 108650, 2020.
- [28] K. He, X. Zhang, S. Ren, and J. Sun, "Deep residual learning for image recognition," pp. 770–778, 2016.
- [29] S. Hochreiter and J. Schmidhuber, "Long short-term memory," *Neural computation*, vol. 9, no. 8, pp. 1735–1780, 1997.
- [30] Z. Wu, T. Yao, Y. Fu, and Y.-G. Jiang, "Deep learning for video classification and captioning," in *Frontiers of multimedia research*, 2017, pp. 3–29.
- [31] A. Ullah, J. Ahmad, K. Muhammad, M. Sajjad, and S. W. Baik, "Action recognition in video sequences using deep bi-directional lstm with cnn features," *IEEE Access*, vol. 6, pp. 1155–1166, 2017.
- [32] K. Simonyan and A. Zisserman, "Very deep convolutional networks for large-scale image recognition," *arXiv preprint arXiv:1409.1556*, 2014.
- [33] C. Szegedy, V. Vanhoucke, S. Ioffe, J. Shlens, and Z. Wojna, "Rethinking the inception architecture for computer vision," in *Proceedings of the IEEE conference on computer vision and pattern recognition*, 2016, pp. 2818–2826.
- [34] J. Deng, W. Dong, R. Socher, L.-J. Li, K. Li, and L. Fei-Fei, "Imagenet: A large-scale hierarchical image database," in *2009 IEEE conference on computer vision and pattern recognition*. Ieee, 2009, pp. 248–255.
- [35] C. Szegedy, W. Liu, Y. Jia, P. Sermanet, S. Reed, D. Anguelov, D. Erhan, V. Vanhoucke, and A. Rabinovich, "Going deeper with convolutions," in *Proceedings of the IEEE conference on computer vision and pattern recognition*, 2015, pp. 1–9.
- [36] M. Lin, Q. Chen, and S. Yan, "Network in network," *arXiv preprint arXiv:1312.4400*, 2013.
- [37] X. Glorot and Y. Bengio, "Understanding the difficulty of training deep feedforward neural networks," in *Proceedings of the thirteenth international conference on artificial intelligence and statistics*, 2010, pp. 249–256.
- [38] Y. LeCun, D. Touresky, G. Hinton, and T. Sejnowski, "A theoretical framework for back-propagation," in *Proceedings of the 1988 connectionist models summer school*, vol. 1. CMU, Pittsburgh, Pa: Morgan Kaufmann, 1988, pp. 21–28.
- [39] D. P. Kingma and J. Ba, "Adam: A method for stochastic optimization," *arXiv preprint arXiv:1412.6980*, 2014.